AIP Advances

RESEARCH ARTICLE | NOVEMBER 19 2026

Nature of hydrogen bond and its lifetime in alkali hydroxides (LiOH, NaOH, KOH) in water

Ruru Ma ; Nitish Baradwaj ; Ken-ichi Nomura ; Rajiv K. Kalia ; Aiichiro Nakano ; Priya Vashishta

Check for updates

AIP Advances 16, 115040 (2026)
https://doi.org/10.1063/5.0310051

View Online
Export Citation

Articles You May Be Interested In

Ion-backscattering study of LiOH-to-Li_2O conversion on a LiH substrate

J. Appl. Phys. (October 1974)

Critical Review of Transport Properties of HCl, KOH, and NaOH in High Temperature Water and Correlations for Transport Properties of H_3O^+ and OH^-

J. Phys. Chem. Ref. Data (May 2023)

Effect of NaOH and precursor concentration on size and magnetic properties of FeCo nanoparticles synthesized using the polyol method

AIP Advances (November 2020)

19 November 2026 22:23:29

AIP Advances
Why Publish With Us?
19 DAYS average time to 1st decision
500+ VIEWS per article (average)
INCLUSIVE scope
Learn More
AIP Publishing

AIP Publishing

Nature of hydrogen bond and its lifetime in alkali hydroxides (LiOH, NaOH, KOH) in water

Cite as: AIP Advances 16, 115040 (2026); doi: 10.1063/5.0310051
Submitted: 31 October 2025 • Accepted: 3 November 2026 •
Published Online: 19 November 2026

View Online Export Citation CrossMark

Ruru Ma, Nitish Baradwaj, Ken-ichi Nomura, Rajiv K. Kalia, Aiichiro Nakano, and Priya Vashishta[a)]

AFFILIATIONS

Collaboratory for Advanced Computing and Simulations, Department of Chemical Engineering and Materials Science, Department of Physics & Astronomy, and Department of Computer Science, University of Southern California, Los Angeles, California 90089-0242, USA

[a)]Author to whom correspondence should be addressed: priyav@usc.edu

ABSTRACT

Hydrogen bonding, its structure, and its lifetime in aqueous solutions of alkali hydroxides (LiOH, NaOH, and KOH) are investigated using quantum molecular dynamics simulations over a concentration range of 1–10 mol. Intermolecular charge density overlap is evaluated using the density functional theory with SCAN *meta*-generalized gradient approximation (meta-GGA) exchange-correlation functional to characterize hydrogen bond interactions. Hydrogen bond lifetime systematically decreases as a function of ionic size from lithium to sodium to potassium. Based on the charge density overlap, the maximum length of the hydrogen bond is found to be 2.1 Å for all the systems. Hydrogen bond lifetimes are computed based on different definitions for each system. Our results based on the H-bond characterized by charge density overlap provide a molecular level understanding of concentration and ion-specific effects on the hydrogen bond network in alkaline aqueous environments.

© 2026 Author(s). All article content, except where otherwise noted, is licensed under a Creative Commons Attribution (CC BY) license (https://creativecommons.org/licenses/by/4.0/). https://doi.org/10.1063/5.0310051

19 November 2026 22:23:29

I. INTRODUCTION

Electrolyte solutions have been gaining increasing importance in a wide variety of scientific and technological fields, ranging from chemical and biological processing[1] to geochemical management and advanced energy storage systems.[2] Their role extends well beyond simple ionic conduction: electrolytes regulate interfacial reactions, enable redox processes, and stabilize charge carriers, thereby acting as a central component in numerous natural and engineered systems. With the global energy transition underway, the demand for safer, cheaper, and higher-performing electrolytes is intensifying, making their study both scientifically and technologically urgent.

Electrochemical energy storage, in particular, has attracted enormous attention because of its ability to provide rapid response, modular scalability, and integration into renewable energy grids.[2] The intermittent nature of solar and wind power requires storage systems capable of delivering electricity on demand, and electrochemical devices, especially rechargeable batteries,[3–8] are among the most viable solutions. Unlike fossil-fuel-based systems, which rely on combustion and mechanical turbines, electrochemical devices directly convert chemical energy into electrical energy, resulting in higher efficiencies and fewer greenhouse gas emissions. This combination of performance and environmental benefit has made rechargeable batteries central to the twenty-first century energy landscape.

Lithium-ion batteries currently dominate the market because of their high energy density, long cycle life, and relatively mature production infrastructure.[9,10] With energy densities[11] ranging from[12–14] 120–220 $\frac{\mathrm{W\ h}}{\mathrm{kg}}$, they are well-suited to portable electronics,[15] electric vehicles, and even aerospace technologies. However, the ever-growing demand for devices, from smartphones[15] to grid-level storage,[16–19] continues to push the limits of lithium resources. Concerns about cost, supply security,[20] and environmental impact have motivated exploration of alternative chemistries.

Sodium-ion batteries offer a promising path forward because sodium is abundant and inexpensive.[21] While their energy density is typically lower than lithium-ion systems, sodium batteries are especially attractive for stationary applications where cost outweighs weight considerations, such as renewable energy integration

© Author(s) 2026

and backup power. Potassium-ion batteries are another emerging technology, notable for their reduced dependence on critical mineral sources[22] and potentially superior ion transport due to the lower solvation energy of K+ ions. In addition, concepts such as sodium–oxygen[23] and potassium–oxygen batteries[24–26] promise even higher theoretical energy densities by coupling alkali metal ions with oxygen redox reactions.

Beyond traditional cation-based storage, research is also advancing into multivalent systems (e.g., Mg2+, Ca2+, and Zn2+), solid-state electrolytes, and hybrid aqueous/organic electrolytes. Each of these designs presents unique challenges in ion mobility, electrode compatibility, and long-term stability. Nevertheless, they collectively highlight the breadth of strategies under development to diversify energy storage beyond lithium.

Amid these developments, a deeper understanding of molecular interactions within electrolytes is critical. Among such interactions, the hydrogen bond, first proposed by Barnal and Fowler in 1933 and pursued by Pauling in 1935,[27–29] plays an outsized role. At its simplest, a hydrogen bond occurs when a hydrogen atom covalently bound to an electronegative atom (donor) interacts with another electronegative atom (acceptor).[30]

In electrochemical systems, hydrogen bonding governs both microscopic and macroscopic behavior. On the molecular scale, hydrogen bonds stabilize solvation shells, dictate ion–solvent coordination numbers, and control solvent reorganization dynamics.[31,32] On the device scale, these interactions impact conductivity, viscosity, electrode–electrolyte interfacial chemistry, and even the stability of the solid–electrolyte interphase (SEI).[33–35] Thus, small changes in hydrogen bond lifetimes or strengths can translate into measurable differences in battery performance.

Water remains the prototypical system for hydrogen bonding studies. Experiments using ultrafast infrared spectroscopy, Raman scattering, and neutron diffraction,[36–40] combined with simulations ranging from classical force fields to *ab initio* molecular dynamics,[41–47] have revealed that water's network is highly dynamic, with bonds continually breaking and reforming on picosecond timescales. These transient interactions explain many of water's anomalies, such as its density maximum at 4 °C, its unusually high boiling point, and its high surface tension.[48,49] Beyond bulk water, hydrogen bonding is crucial in nanoscience,[50] where it stabilizes molecular assemblies[51,52] and defines vibrational fingerprints used to probe surface chemistry.[53]

Despite this wealth of knowledge, much less is known about hydrogen bonding in mixed solvent or salt-rich environments, such as those found in battery electrolytes.[54–57] The presence of ions perturbs the local hydrogen bond network, modifies solvent orientation, and creates competition between ion–dipole and hydrogen bond interactions. For example, lithium ions strongly coordinate with solvent oxygen atoms, effectively replacing hydrogen bonds with ion–solvent interactions. By contrast, larger ions such as sodium and potassium, due their larger size than hydrogen, may alter the coordination shell and impact the hydrogen bonding network, albeit with altered geometries and lifetimes. Understanding these subtleties is essential for predicting ion mobility and, by extension, device performance.

Traditional approaches to hydrogen bond characterization rely on geometrical criteria, such as donor–acceptor distance thresholds and angular cutoffs. While widely used, these definitions are somewhat arbitrary and can yield inconsistent results across different systems. Moreover, geometric criteria do not fully capture the electronic origin of hydrogen bonds, which are fundamentally rooted in electron density redistribution.

To address these limitations, we employ charge density overlap as a more physically grounded metric. By analyzing regions where the electron density associated with a donor hydrogen atom overlaps significantly with that of an acceptor atom, this method captures the essence of hydrogen bonding without reliance on ad hoc geometrical cutoffs. Charge density analysis has the added advantage of connecting directly to quantum-mechanical descriptions of bonding, making it a robust framework for comparing different electrolytes on equal footing.

In addition to static analysis, it is critical to assess the dynamics of hydrogen bonds. Hydrogen bonds are inherently transient, with lifetimes that depend on temperature, pressure, and local environment. We therefore calculate lifetimes using multiple definitions, including continuous and intermittent correlation functions, to evaluate the robustness of our conclusions. This dual strategy of combining charge density overlap with lifetime analysis enables a comprehensive characterization of hydrogen bonding in lithium, sodium, and potassium electrolytes.

II. METHOD

Quantum molecular dynamics (QMD) simulations[58] are performed using the Vienna *Ab initio* Simulation Package (VASP) software.[59] The electronic states are calculated using the projector augmented-wave (PAW) method[60] in the framework of density functional theory (DFT).[61,62] The exchange-correlation effects are incorporated using the SCAN functional.[63]

We initiate the simulations using a bulk water configuration previously established, consisting of 108 H_2O molecules.[64,65] To construct alkali hydroxide solutions at specified concentrations, a selected number of water molecules are randomly chosen, and in each system, one hydrogen atom is substituted by a cation M $(M \in \{Li, Na, K\})$. The simulation box dimensions are subsequently adjusted to match the experimental density, followed by geometry relaxation to obtain a locally minimized energy configuration.[65]

Following the construction of the initial configuration, the system is first equilibrated via QMD simulations in the canonical (NVT) ensemble at 303 K. The procedure consists of 1000 steps for 0.4 ps using a time step of 0.4 fs, followed by extended NVT thermalization of 20 000 steps for 8 ps. To generate a configuration at room temperature, we then thermalize the systems in a microcanonical (NVE) ensemble for 2 ps with a time step of 0.25 fs. Subsequently, structural and vibrational correlation functions are computed from a 5 ps microcanonical MD trajectory of 20 000 steps with a 0.25 fs time step.

III. COMPARISON WITH NEUTRON SCATTERING EXPERIMENTS ON 17 MOL NaOD IN WATER

To assess the quality of our simulations and validate our results, we compare the calculated structural features with experimental data from a neutron-scattering study on 17 mol NaOD aqueous solution by Semrouni *et al.*[66]

19 November 2026 22:23:29

© Author(s) 2026

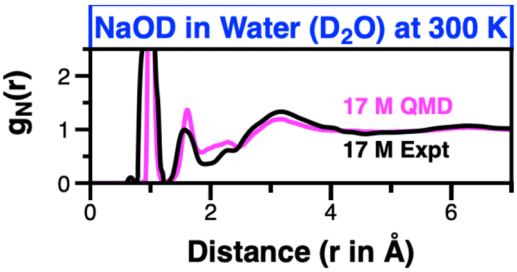


FIG. 1. Neutron pair distribution function $g_N(r)$, which is the neutron cross section weighted pair distribution function $g(r)$, of 17M NaOH in water solution at 300 K. The magenta line is the simulation of $g_N(r)$. The black line is experimental $g_N(r)$, obtained from Ref. 66. Reproduced with permission from Semrouni *et al.*, Phys. Chem. Chem. Phys. **21**(13), 6828–6838 (2019). Copyright 1999 Royal Society of Chemistry.

Figure 1 presents the calculated $g_N(r)$,[67] which is the neutron cross section weighted pair distribution function $g(r)$, where the magenta curve corresponds to the simulation and the black curve represents the experimental[66] data. The close agreement between simulation and experimental results supports the accuracy and validity of our simulations for concentrated hydroxide solutions.[65] It should be pointed out here that in QMD simulations, $g(r)$ is computed directly in r-space, whereas in the 2019 neutron experiment by Semrouni *et al.*, $g_N(r)$ was obtained by Fourier transforming a finite k-range data into r-space. A small peak in experimental $g_N(r)$ at about 0.7 Å, which is an error because there are no bonds shorter than the D-O covalent bond, is a manifestation of this error in Fourier transformation due to limited range k-space data.

IV. RESULTS

According to Pimentel and McClellan's criteria of hydrogen bonds,[68] a hydrogen bond should satisfy two things: (a) there is a bond between two atoms; (b) a hydrogen atom that is already covalently bonded with another atom is involved. The large variation in computed hydrogen bond lifetimes across different definitions primarily arises from differences in geometric constraints and the sensitivity of time correlation functions to those criteria. For example, Wernet *et al.*,[31] employed a nonlinear angle-dependent cutoff involving both O···O distance and O–H bond orientation, which tends to capture longer-lived hydrogen bonds. In contrast, the room temperature water (RTW) definition is based on stricter instantaneous geometric thresholds, leading to shorter lifetimes used by Kumar *et al.*[71] These different criteria for H-bonds highlight the limitations of purely geometric approaches and motivate the use of electronic structure-based metrics such as charge density overlap. The criteria based on charge density overlap provide a clear chemical characterization of the hydrogen bond. In the following, we describe the nature of hydrogen bonds with charge density overlap computed within the SCAN-DFT framework. The charge density in the middle of the covalent O–H bond is 0.45 electrons/Å^3. **We define the threshold for the existence of a hydrogen bond to be 2.1Å where the charge density overlap is less than 0.006 electrons/Å^3.**

We show in Fig. 2 the hydrogen bond configurations of 1.05M LiOH in water solution at 300 K. Figure 2(a) shows two H_2O

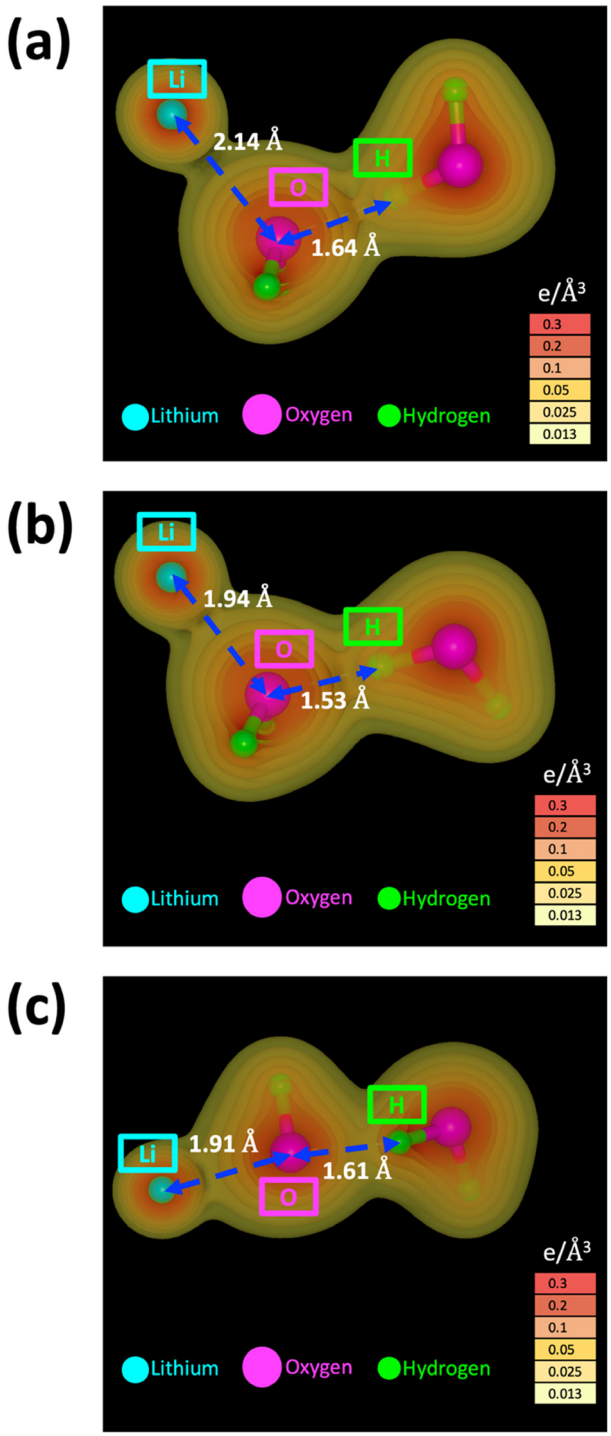


FIG. 2. Hydrogen bond configurations of 1.05M LiOH in water solution at 300 K. (a) Two H_2O molecules and one Li ion at an O···H distance of 1.64 Å and charge density overlap between O and Li at 2.14.44M Å. (b) Two H_2O molecules and one Li ion at an O···H distance of 1.53 Å and O···Li at a distance of 1.94 Å. (c) One H_2O, one Li, and one OH ion at an O···H distance of 1.61 Å and O···Li at a distance of 1.91 Å.

19 November 2026 22:23:29

© Author(s) 2026

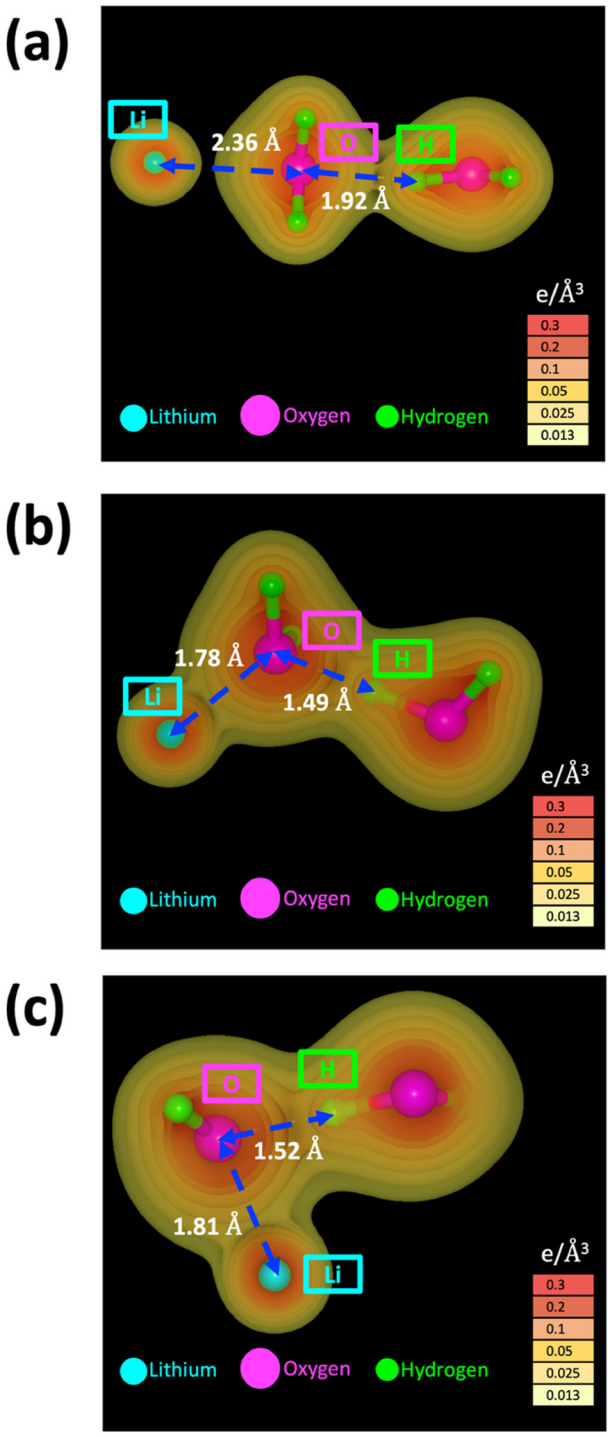


FIG. 3. Hydrogen bond configurations of 9.66M LiOH in water solution at 300 K. (a) Two H_2O molecules and one Li ion at an O· · ·H distance of 1.92 Å and there is no charge density overlap between O and Li at a distance of 2.36 Å. (b) Two H_2O molecules and one Li ion at an O· · ·H distance of 1.49 Å and O· · ·Li at a distance of 1.78 Å. (c) One H_2O, one Li, and one OH ion at an O· · ·H distance of 1.52 Å and O· · ·Li at a distance of 1.81 Å.

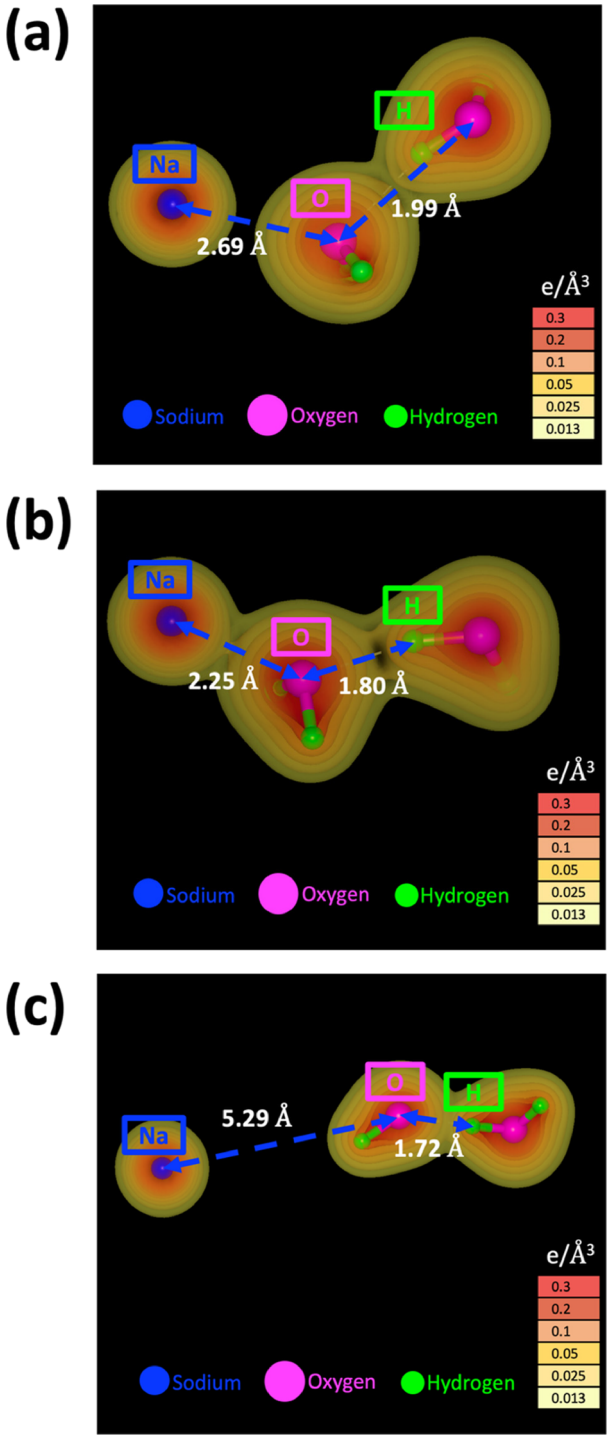


FIG. 4. Hydrogen bond configurations of 1.05 M NaOH in water solution at 300 K. (a) Two H_2O molecules and one Na ion at an O· · ·H distance of 1.99 Å and there is no charge density overlap between O and Na at a distance of 2.69 Å. (b) Two H_2O molecules and one Na ion at an O· · ·H distance of 1.80 Å and O· · ·Na at a distance of 2.25 Å. (c) One H_2O, one Na, and one OH ion at an O· · ·H distance of 1.72 Å and there is no bond between Na and O at a distance of 5.29 Å.

19 November 2026 22:23:29

© Author(s) 2026

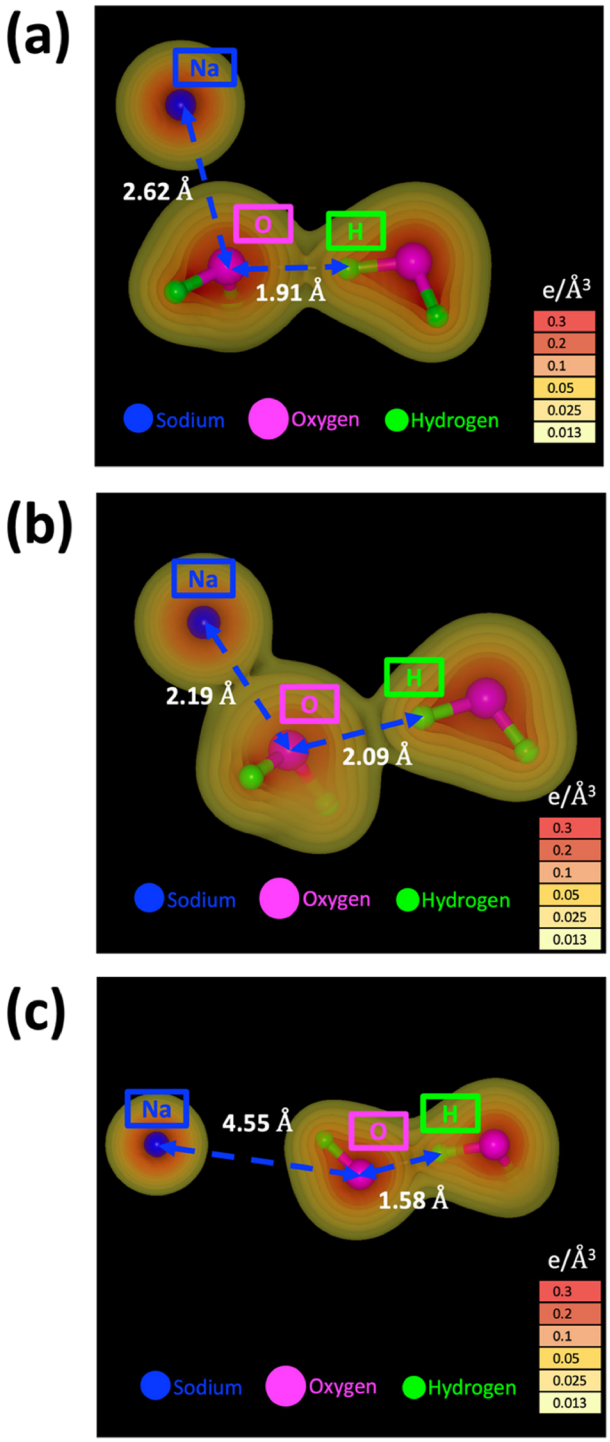


FIG. 5. Hydrogen bond configurations of 9.66M NaOH in water solution at 300 K. (a) Two H_2O molecules and one Na ion at an O· · ·H distance of 1.91 Å and no charge density overlap between O and Na at a distance of 2.62 Å. (b) Two H_2O molecules and one Na ion at an O· · ·H distance of 2.09 Å and O· · ·Na at a distance of 2.19 Å. (c) One H_2O, one Na, and one OH ion at an O· · ·H distance of 1.58 Å and there is no bond between Na and O at a distance of 4.55 Å.

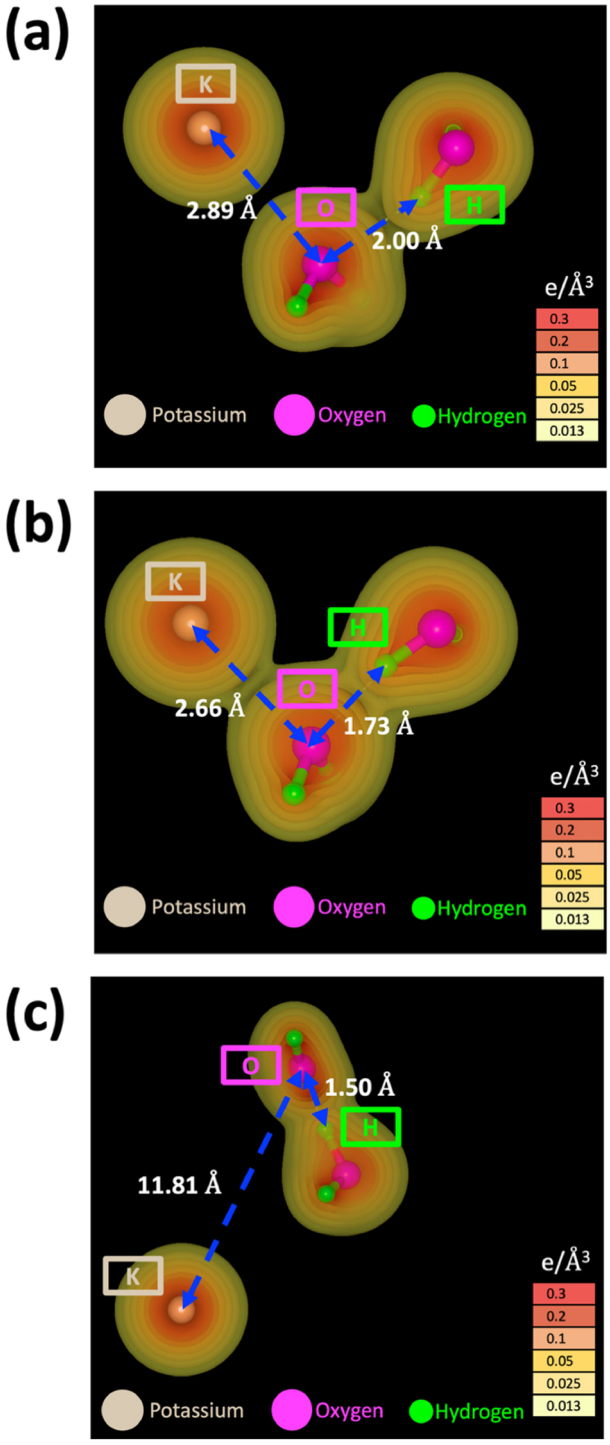


FIG. 6. Hydrogen bond configurations of 1.05 M KOH in water solution at 300 K. (a) Two H_2O molecules and one K ion at an O· · ·H distance of 2.0 Å and there is no charge density overlap between O and K at a distance of 2.89 Å. (b) Two H_2O molecules and one K ion at an O· · ·H distance of 1.73 Å and O· · ·K at a distance of 2.66 Å. (c) One H_2O, one K, and one OH ion at an O· · ·H distance of 1.50 Å and there is no charge density overlap between K and O at a distance of 11.81 Å.

19 November 2026 22:23:29

© Author(s) 2026

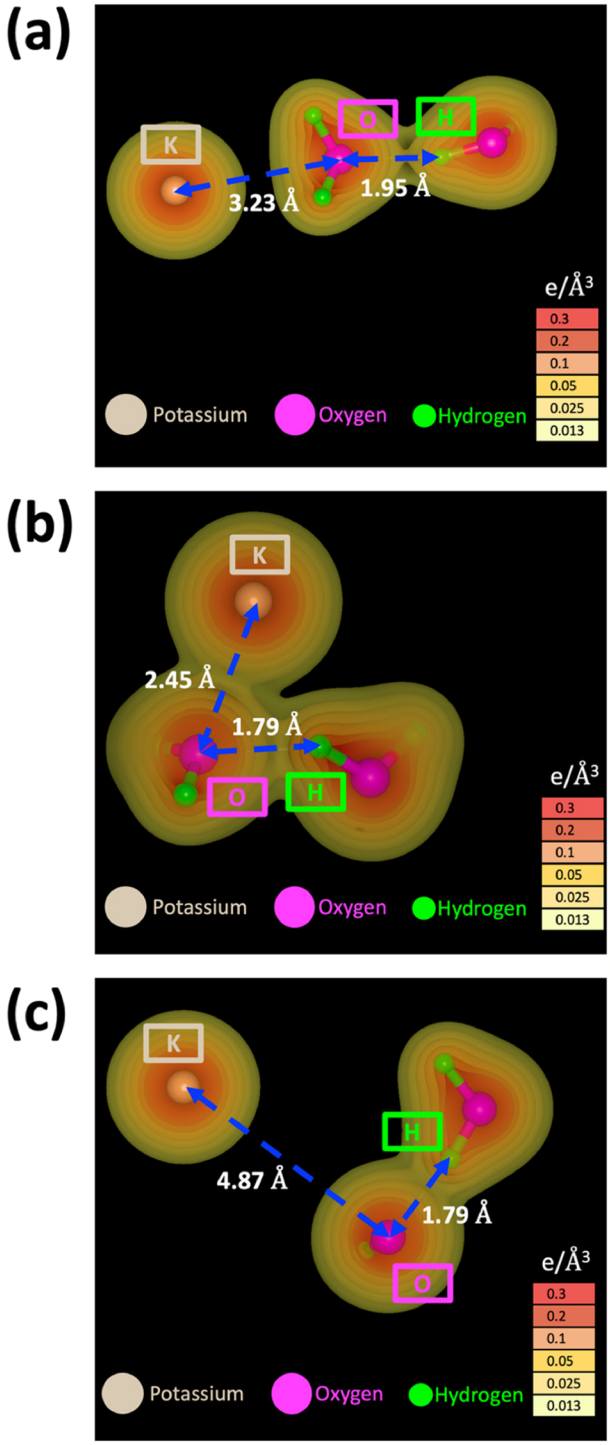


FIG. 7. Hydrogen bond configurations of 9.66 M KOH in water solution at 300 K. (a) Two H_2O molecules and one K ion at an O· · ·H distance of 1.95 Å and there is no charge density overlap between O and K at a distance of 3.23 Å. (b) Two H_2O molecules and one K ion at an O· · ·H distance of 1.79 Å and O· · ·K at a distance of 2.45 Å. (c) One H_2O, one K, and one OH ion at an O· · ·H distance of 1.79 Å and there is no charge density overlap between K and O at a distance of 4.87 Å.

molecules and one Li ion at an O· · ·H distance of 1.64 Å. Figure 2(b) shows two H_2O molecules and one Li ion at an O· · ·H distance of 1.53 Å. O· · ·Li is at a distance of 1.94 Å. Figure 2(c) shows one H_2O, one Li, and one OH ion at an O· · ·H distance of 1.61 Å. O· · ·Li is at a distance of 1.91 Å. Similarly, Figs. 3–7 show hydrogen bond configurations of 1.05M and 9.66M of MOH (M ∈ {Li, Na, K}), giving detailed data from charge density analysis. In all the systems investigated here, we find the maximum length of the hydrogen bond to be 2.1 Å.

To gain a robust understanding of hydrogen bonding in water where H_2O molecules are broken because of ionic substitution by Li, Na, and K, we examine the partial pair distribution functions, $g_{OH}(r)$ and $g_{HO}(r)$, to determine the surroundings of O and H, respectively. This allows unambiguous determination of the covalent bonds and H-bonds in the system. This is shown in Figs. 8–10. The red arrows in $g_{OH}(r)$ and $g_{HO}(r)$ give the coordination numbers $n_{OH}(r_0)$ and $n_{HO}(r_0)$ at a distance of r_0 = 2.1 Å, respectively. This is all the information that we need to determine the total number of H-bonds in the system. For ice, there are two H-bonds for each oxygen and one H-bond for each hydrogen, making each water molecule tetrahedrally coordinated, corresponding to 100% hydrogen bonding. For pure water, at room temperature,[69] $n_{OH}(r_0 = 2.1\ \text{Å})$ is 3.8, giving the number of H-bonds to be 3.8 − 2 = 1.8. Similarly, for hydrogen, $n_{HO}(r_0 = 2.1\ \text{Å})$ is 1.9, giving the number of H-bonds to be 1.9 − 1 = 0.9. Therefore, for one water molecule, there are 1.8 + 2 × 0.9 = 3.6 H-bonds. This atomistic approach based on the partial pair distribution function is necessary when dealing with broken water molecules as a result of Li, Na, and K substitution. In addition, this approach does not involve any geometric consideration and only requires the maximum distance of charge density overlap r_0.

The nearest neighbor (NN) coordination number of O–H $n_{OH}(r)$ at r_0 = 2.1 Å is a sum of the number of covalent bonds (NCB) and the number of hydrogen bonds (NHB), $n_{OH}(r_0) = NCB + NHB$. As a confirmation, it is also verified from the coordination number of O to nearest covalently bonded H at distances less than 1.2 Å. It should be noted that the number of covalent bonds is consistent with the concentration of LiOH, NaOH, and KOH in water. The number of hydrogen bonds decreases as the number of MOH (M ∈ {Li, Na, K}) increases in the solution (Fig. 11).

The total number of H-bonds formed by oxygen in the system is computed as the number of oxygen atoms multiplied by the H-bonds per oxygen, as shown in Table I.

The total number of H-bonds formed by hydrogen in the system is computed as the number of hydrogen atoms multiplied by the H-bonds per hydrogen, as shown in Table II.

As shown in Table III, the total number of H-bonds in the system is computed as the number of oxygen atoms multiplied by the number of H-bonds plus the total number of hydrogen atoms multiplied by the number of H-bonds.

Hydrogen bond lifetimes depend on how the hydrogen bond is defined. We define the H-bond using the definition of charge density overlap.

Following our charge density overlap definition of the H-bond, we determine the length of the H-bond to be 2.1 Å for all the systems studied in this work.

We compute the hydrogen bond population correlation function $C^{HB}(t)$ using the definition of existence of the H-bond,

19 November 2026 22:23:29

© Author(s) 2026

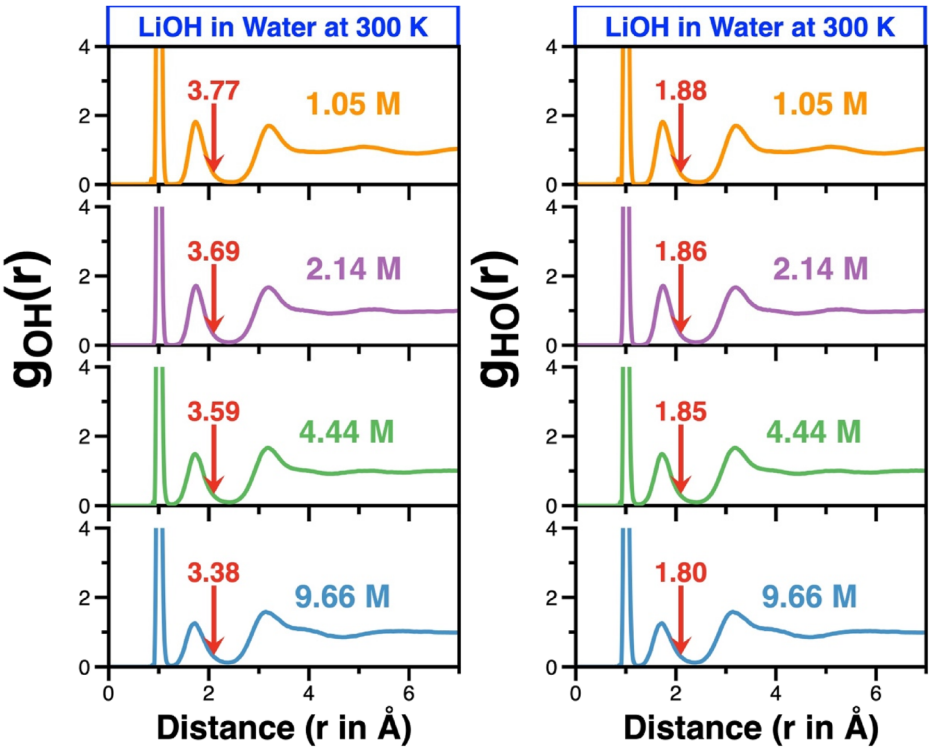


FIG. 8. Partial pair distribution functions $g_{OH}(r)$ and $g_{HO}(r)$ of LiOH in water solution at 300 K. 1.05 M: orange; 2.14 M: purple; 4.44 M: green; 9.66 M: blue. Numerals are coordination numbers at r_0 = 2.1 Å marked by red arrows.

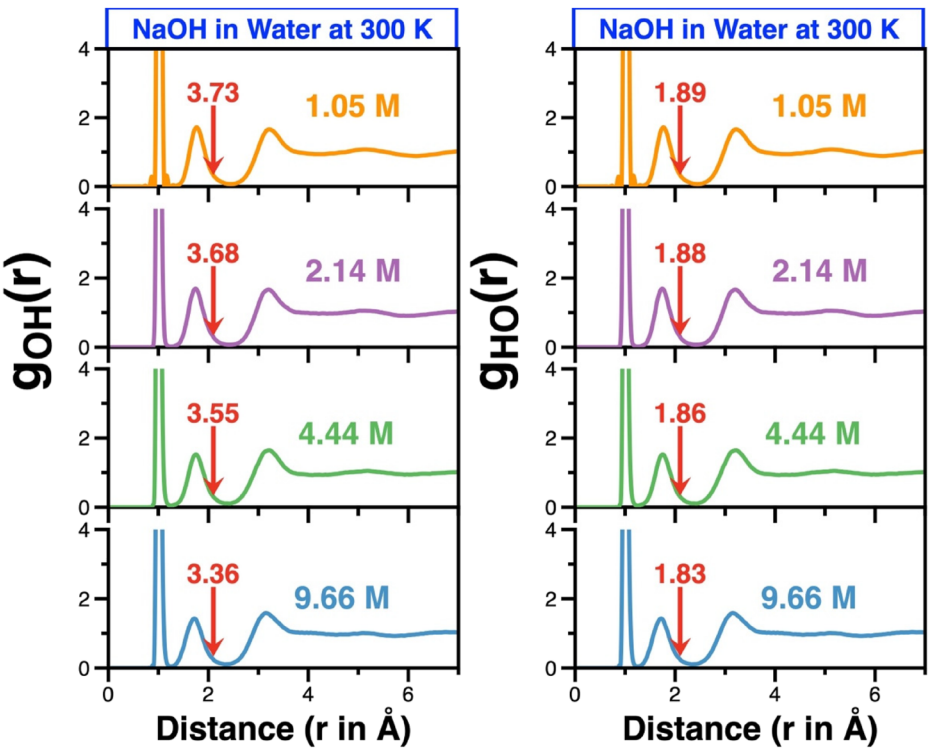


FIG. 9. Partial pair distribution functions $g_{OH}(r)$ and $g_{HO}(r)$ of NaOH in water solution at 300 K. 1.05 M: orange; 2.14 M: purple; 4.44 M: green; 9.66 M: blue. Numerals are coordination numbers at r_0 = 2.1 Å marked by red arrows.

19 November 2026 22:23:29

© Author(s) 2026

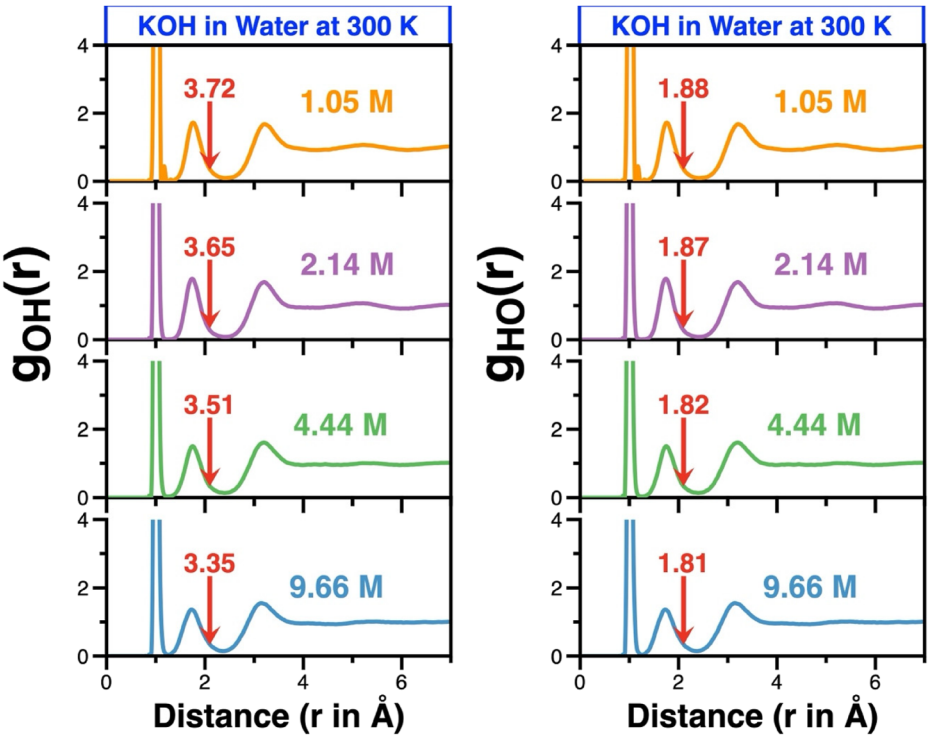


FIG. 10. Partial pair distribution functions $g_{OH}(r)$ and $g_{HO}(r)$ of KOH in water solution at 300 K. 1.05 M: orange; 2.14 M: purple; 4.44 M: green; 9.66 M: blue. Numerals are coordination numbers at r_0 = 2.1 Å marked by red arrows.

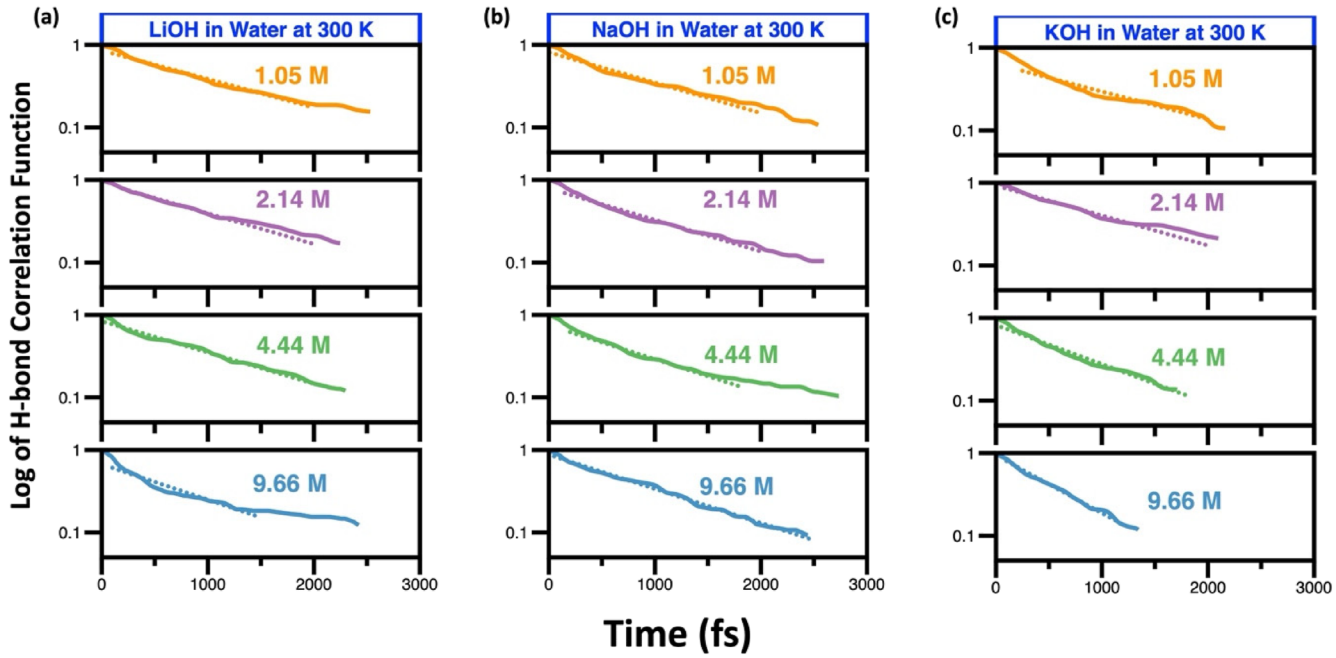


FIG. 11. Hydrogen bond lifetime of LiOH (a), NaOH (b), and KOH (c) in water solution at 300 K: Log of H-bond correlation function vs time, based on our charge density overlap criterion, where the maximum O· · ·H distance is set to r_{OH} = 2.1 Å. 1.05 M: orange; 2.14 M: purple; 4 M: green; 9.66 M: blue.

19 November 2026 22:23:29

© Author(s) 2026

TABLE I. The detailed values of coordination numbers $n_{OH}(r_0 = 2.1\ \text{Å})$ for all the systems are summarized.

Systems	NN coordination of O–H $n_{\text{OH}}(r_0 = 2.1\ \text{Å})$	Number of covalent bonds for each O	Number of hydrogen bonds for each O	Number of O atoms in our system	Total number of H-bonds for O in our system
Ice	**4**	**2**	**2**	**108**	**216**
H_2O	**3.8**	**2**	**1.8**	**108**	**194.4**
1.05M LiOH	**3.77**	**1.98**	**1.79**	**108**	**193.32**
2.14M LiOH	**3.69**	**1.96**	**1.73**	**108**	**186.84**
4.44M LiOH	**3.59**	**1.93**	**1.66**	**108**	**179.28**
9.66M LiOH	**3.38**	**1.85**	**1.53**	**108**	**165.24**
1.05M NaOH	**3.73**	**1.98**	**1.75**	**108**	**189**
2.14M NaOH	**3.68**	**1.96**	**1.72**	**108**	**185.76**
4.44M NaOH	**3.55**	**1.93**	**1.62**	**108**	**174.96**
9.66M NaOH	**3.36**	**1.85**	**1.51**	**108**	**163.08**
17.0M NaOH	**3.14**	**1.77**	**1.37**	**108**	**147.96**
1.05M KOH	**3.72**	**1.98**	**1.74**	**108**	**187.92**
2.14M KOH	**3.65**	**1.96**	**1.69**	**108**	**182.52**
4.44M KOH	**3.51**	**1.93**	**1.58**	**108**	**170.64**
9.66M KOH	**3.35**	**1.85**	**1.5**	**108**	**162**

TABLE II. The detailed values of coordination numbers $n_{HO}(r_0 = 2.1\ \text{Å})$ for all the systems are summarized.

Systems	NN coordination of H–O $n_{\text{HO}}(r_0 = 2.1\text{Å})$	Number of covalent bonds for each H	Number of hydrogen bonds for each H	Number of H atoms in our system	Total number of H-bonds for H in our system
Ice	**2**	**1**	**1**	**216**	**216**
H_2O	**1.9**	**1**	**0.9**	**216**	**194.4**
1.05M LiOH	**1.88**	**0.9907**	**0.89**	**214**	**190.46**
2.14M LiOH	**1.86**	**0.9814**	**0.88**	**212**	**186.56**
4.44M LiOH	**1.85**	**0.963**	**0.88**	**208**	**183.04**
9.66M LiOH	**1.80**	**0.926**	**0.87**	**200**	**174.00**
1.05M NaOH	**1.89**	**0.9907**	**0.89**	**214**	**190.46**
2.14M NaOH	**1.88**	**0.9814**	**0.89**	**212**	**188.68**
4.44M NaOH	**1.86**	**0.963**	**0.89**	**208**	**185.12**
9.66M NaOH	**1.83**	**0.926**	**0.89**	**200**	**178.00**
17.0M NaOH	**1.78**	**0.884**	**0.89**	**191**	**169.99**
1.05M KOH	**1.88**	**0.9907**	**0.89**	**214**	**190.46**
2.14M KOH	**1.87**	**0.9814**	**0.88**	**212**	**186.56**
4.44M KOH	**1.82**	**0.963**	**0.86**	**208**	**178.88**
9.66M KOH	**1.81**	**0.926**	**0.88**	**200**	**176.00**

$$C^{HB}(t) = \frac{1}{N_{HB}^{t=0}} \sum_{i=1}^{N} \sum_{j<i}^{N} \langle h_{ij}(0) h_{ij}(t) \rangle, \tag{1}$$

where $N_{HB}^{t=0}$ is the number of hydrogen bonds at time $t = 0$ and $h_{ij}(t)$ is 1 if a hydrogen bond exists between atoms i and j at time t, and zero otherwise.[70] To facilitate linear fitting, we use the logarithm of the correlation function. Our computed values are shown in Table IV.

We have also computed H-bond lifetimes using the following three definitions from the literature:

A. According to Kumar *et al.*,[71] a hydrogen bond exists if the angle–distance definition satisfies the condition

$$r_{\text{OH}} < C_{\text{OH}}^1 + C_{\text{OH}}^2 \cos\theta, \tag{2}$$

where r_{OH} is the intermolecular O···H distance, θ is the angle between the donor oxygen and the two hydrogen atoms

19 November 2026 22:23:29

© Author(s) 2026

TABLE III. Total number of H-bonds for oxygen and hydrogen along with total number of H-bonds in the system is given below.

Systems	Total number of H-bonds for O in our system	Total number of H-bonds for H in our system	Total number of H-bonds in our system
Ice	**216**	**216**	**432**
H_2O	**194.4**	**194.4**	**388.8**
1.05M LiOH	**193.32**	**190.46**	**383.78**
2.14M LiOH	**186.84**	**186.56**	**373.40**
4.44M LiOH	**179.28**	**183.04**	**362.32**
9.66M LiOH	**165.24**	**174.00**	**339.24**
1.05M NaOH	**189**	**190.46**	**379.46**
2.14M NaOH	**185.76**	**188.68**	**374.44**
4.44M NaOH	**174.96**	**185.12**	**360.08**
9.66M NaOH	**163.08**	**178.00**	**341.08**
17.0M NaOH	**147.96**	**169.99**	**317.95**
1.05M KOH	**187.92**	**190.46**	**378.38**
2.14M KOH	**182.52**	**186.56**	**369.08**
4.44M KOH	**170.64**	**178.88**	**349.52**
9.66M KOH	**162.00**	**176.00**	**338.00**

TABLE IV. Hydrogen bond lifetime based on our charge density overlap criterion, where the maximum O···H distance is set to r_{OH} = 2.1 Å.

System	τ (picoseconds)
H_2O	**1.32**
1.05 M LiOH	**1.26**
2.14 M LiOH	**1.17**
4.44 M LiOH	**1.15**
9.66 M LiOH	**1.01**
1.05 M NaOH	**1.18**
2.14 M NaOH	**1.14**
4.44 M NaOH	**1.06**
9.66 M NaOH	**1.05**
17 M NaOH	**0.59**
1.05 M KOH	**1.30**
2.14 M KOH	**1.20**
4.44 M KOH	**0.92**
9.66 M KOH	**0.62**

(one inter- and one intra-molecular), and C^1_{OH} and C^2_{OH} are phase-dependent parameters.

C^1_{OH} = 1.37 Å and C^2_{OH} = −1.71 Å for room temperature water.[71]

B. According to Todorova[28] and Kuo *et al.*,[30] a hydrogen bond exists if the geometric cutoff definition satisfies the following conditions.

(B 1) Todorova *et al.* defined a hydrogen bond as O···O distance < 3.5 Å and O–H···O angle > 135°.[28]

(B 2) *Kuo et al.* defined a hydrogen bond as O···H distance between 1.59 and 2.27 Å and O–H···O angle > 140°.[30]

C. According to Wernet *et al.*,[31] a hydrogen bond exists if the distance–angle definition satisfies the following condition:

$$r(\theta) < -0.000\ 44\theta^2 + 3.3, \tag{4}$$

where $r(\theta)$ is the oxygen-oxygen distance and θ is the angle between the O···O vector and the O–H bond direction.[31]

The hydrogen bond lifetimes calculated using the definitions (A-C) from the literature are given in the supplementary material, along with the log plots of population time.

V. SUMMARY

We have carried out exhaustive electronic structure calculations to determine the charge density overlap in alkali hydroxides (LiOH, NaOH, and KOH) using quantum molecular dynamics simulations for a wide range of solute concentration between 1 and 10 mol to determine hydrogen bond lifetimes. We have validated our calculated structural properties with available neutron data on 17 mol NaOD in D_2O. Our results demonstrate that charge density overlap-based analysis provides a clear and consistent physically meaningful framework for characterizing hydrogen bonds in aqueous and electrolyte environments. Unlike traditional geometric definitions, which depend on arbitrary cutoffs and may fail under highly perturbed conditions, the charge density overlap approach is robust and directly reflects the underlying electronic interactions governing hydrogen bonding. Our proposed framework not only reconciles discrepancies among conventional criteria but also offers a unified picture linking molecular structure, solvation dynamics, and ion-induced perturbations in hydrogen bond networks. By bridging geometric and electronic perspectives, this methodology establishes a foundation for quantitatively comparing hydrogen bonding across diverse chemical systems, paving the way for more accurate modeling of electrolyte and interfacial phenomena. We are currently planning neutron-scattering experiments on alkali hydroxide (LiOH, NaOH, and KOH) systems using these *ab initio* data as a guidance.

A more complete understanding of hydrogen bonding will not only enrich the basic science of electrolyte solutions but also guide the rational design of next-generation batteries. By identifying how microscopic interactions control macroscopic behavior, researchers can optimize electrolytes for stability, safety, and performance, helping to meet the world's growing energy demands in a sustainable manner.

SUPPLEMENTARY MATERIAL

The hydrogen bond lifetimes calculated using the definitions (A–C in Sec. IV) from the literature are given in the supplementary material, along with the log plots of population time.

ACKNOWLEDGMENTS

This research was supported by the U.S. Department of Energy, Office of Basic Energy Sciences, Division of Materials Sciences and Engineering, Neutron Scattering and Instrumentation Sciences Program, under Award No. DE-SC0023146.

19 November 2026 22:23:29

© Author(s) 2026

AUTHOR DECLARATIONS

Conflict of Interest

The authors have no conflicts to disclose.

Author Contributions

Ruru Ma: Formal analysis (equal); Investigation (equal); Visualization (equal); Writing – original draft (equal); Writing – review & editing (equal). **Nitish Baradwaj**: Data curation (equal); Formal analysis (equal); Investigation (equal); Methodology (equal); Software (equal); Validation (lead); Visualization (equal); Writing – original draft (lead); Writing – review & editing (lead). **Ken-ichi Nomura**: Software (equal); Supervision (equal); Writing – review & editing (equal). **Rajiv K. Kalia**: Funding acquisition (equal); Writing – review & editing (equal). **Aiichiro Nakano**: Funding acquisition (equal); Resources (equal); Writing – review & editing (equal). **Priya Vashishta**: Conceptualization (lead); Funding acquisition (lead); Project administration (lead); Resources (lead); Writing – review & editing (equal).

DATA AVAILABILITY

The data that support the findings of this study are available from the corresponding author upon reasonable request.

REFERENCES

[1] R. Beudert, H. Bertagnolli, and M. Zeller, J. Chem. Phys. **106**(21), 8841–8848 (1997).
[2] Z. Yu, J. Xiongjie, Y. Cai, R. Su, Q. Zhu, T. Zhao, and H. Jiang, Energy Storage Mater. **69**, 103404 (2024).
[3] S. Aberoumand, P. Woodfield, B. Shabani, and D. V. Dao, Phys. Rep. **881**, 1–49 (2020).
[4] A. G. Olabi, T. Wilberforce, E. T. Sayed, A. G. Abo-Khalil, H. M. Maghrabie, K. Elsaid, and M. A. Abdelkareem, Energy **254**, 123987 (2022).
[5] G. J. May, A. Davidson, and B. Monahov, J. Energy Storage **15**, 145–157 (2018).
[6] X. Shi, Y. Dai, O. C. Esan, X. Huo, L. An, and T. Zhao, ACS Appl. Mater. Interfaces **13**(41), 48795–48800 (2021).
[7] X. Shi, X. Huo, O. C. Esan, L. An, and T. S. Zhao, Appl. Energy **297**, 117145 (2021).
[8] J. Xue, S. Deng, R. Wang, and Y. Li, Carbon **205**, 422–434 (2023).
[9] J. Panpage, K. Shi, H. Wu, J. Li, R. Zhang, Q. Liu, and Z. Liang, Adv. Energy Mater. **14**(4), 2302862 (2023).
[10] G. Jiang, W. Zou, W. Zhang, Z. Ou, S. Qi, T. Ma, Z. Cui, Z. Liang, and L. Du, Adv. Energy Mater. **14**(12), 2303672 (2024).
[11] A. M. Ralls, K. Leong, J. Clayton, P. Fuelling, C. Mercer, V. Navarro, and P. L. Menezes, Materials **16**(17), 6063 (2023).
[12] J. W. Choi and D. Aurbach, Nat. Rev. Mater. **1**(4), 16013 (2016).
[13] J. Li, Z. Du, R. E. Ruther, S. J. An, L. A. David, K. Hays, M. Wood, N. D. Phillip, Y. Sheng, C. Mao, S. Kalnaus, C. Daniel, and D. L. Wood, JOM **69**(9), 1484–1496 (2017).
[14] X. Shen, H. Liu, X.-B. Cheng, C. Yan, and J.-Q. Huang, Energy Storage Mater. **12**, 161–175 (2018).
[15] J. M. Tarascon and M. Armand, Nature **414**(6861), 359–367 (2001).
[16] Z. Liu, J. Song, J. Kubal, N. Susarla, K. W. Knehr, E. Islam, P. Nelson, and S. Ahmed, Energy Policy **158**, 112564 (2021).
[17] M. Knez, G. K. Zevnik, and M. Obrecht, Renewable Sustainable Energy Rev. **109**, 284–293 (2019).
[18] I. Sotnyk, D. Hulak, O. Yakushev, O. Yakusheva, O. V. P. Prokopenko, and A. Yevdokymov, Polityka Energetyczna—Energy Policy J. **23**(3), 147–164 (2020).
[19] S. Hardman, K. L. Fleming, E. Khare, and M. M. Ramadan, MIT Sci. Policy Rev. **2**, 46 (2021).
[20] C. P. Grey and D. S. Hall, Nat. Commun. **11**(1), 6279 (2020).
[21] A. Yao, S. M. Benson, and W. C. Chueh, Nat. Energy **10**(3), 404–416 (2025).
[22] S. Dhir, J. Cattermull, B. Jagger, M. Schart, L. F. Olbrich, Y. Chen, J. Zhao, K. Sada, A. Goodwin, and M. Pasta, Nat. Commun. **15**(1), 7580 (2024).
[23] J. Lu, Y. J. Lee, X. Luo, K. C. Lau, M. Asadi, H. H. Wang, S. Brombosz, J. Wen, D. Zhai, Z. Chen, D. J. Miller, Y. S. Jeong, J. B. Park, Z. Z. Fang, B. Kumar, A. Salehi-Khojin, Y. K. Sun, L. A. Curtiss, and K. Amine, Nature **529**(7586), 377–382 (2016).
[24] P. Hartmann, C. L. Bender, M. Vračar, A. K. Dürr, A. Garsuch, J. Janek, and P. Adelhelm, Nat. Mater. **12**(3), 228–232 (2013).
[25] P. Hartmann, C. L. Bender, J. Sann, A. K. Dürr, M. Jansen, J. Janek, and P. Adelhelm, Phys. Chem. Chem. Phys. **15**(28), 11661–11672 (2013).
[26] X. Ren and Y. Wu, J. Am. Chem. Soc. **135**(8), 2923–2926 (2013).
[27] J. D. Bernal and R. H. Fowler, J. Chem. Phys. **1**(8), 515–548 (1933).
[28] T. Todorova, A. P. Seitsonen, J. Hutter, I. F. W. Kuo, and C. J. Mundy, J. Phys. Chem. B **110**(8), 3685–3691 (2006).
[29] L. Pauling, J. Am. Chem. Soc. **57**(12), 2680–2684 (1935).
[30] I.-F. W. Kuo and C. J. Mundy, Science **303**(5658), 658–660 (2004).
[31] P. Wernet, D. Nordlund, U. Bergmann, M. Cavalleri, M. Odelius, H. Ogasawara, L. A. Näslund, T. K. Hirsch, L. Ojamäe, P. Glatzel, L. G. M. Pettersson, and A. Nilsson, Science **304**(5673), 995–999 (2004).
[32] T. Sun, Q. Nian, X. Ren, and Z. Tao, Joule **7**(12), 2700–2731 (2023).
[33] Z. Lin, H.-Y. Shi, L. Lin, X. Yang, W. Wu, and X. Sun, Nat. Commun. **12**(1), 4424 (2021).
[34] L. Sieuw, A. Jouhara, É. Quarez, C. Auger, J.-F. Gohy, P. Poizot, and A. Vlad, Chem. Sci. **10**(2), 418–426 (2019).
[35] L. Li, M.-F. Lin, X. Zhang, A. Britz, A. Krishnamoorthy, R. Ma, R. K. Kalia, A. Nakano, P. Vashishta, P. Ajayan, M. C. Hoffmann, D. M. Fritz, U. Bergmann, and O. V. Prezhdo, Nano Lett. **19**(9), 6078–6086 (2019).
[36] H. J. Bakker and J. L. Skinner, Chem. Rev. **110**(3), 1498–1517 (2010).
[37] Y. L. A. Rezus and H. J. Bakker, J. Chem. Phys. **123**(11), 114502 (2005).
[38] J. D. Eaves, J. J. Loparo, C. J. Fecko, S. T. Roberts, A. Tokmakoff, and P. L. Geissler, Proc. Natl. Acad. Sci. U. S. A. **102**(37), 13019–13022 (2005).
[39] M. D. Fayer, Annu. Rev. Phys. Chem. **60**, 21–38 (2009).
[40] M. D. Fayer and N. E. Levinger, Annu. Rev. Anal. Chem. **3**, 89–107 (2010).
[41] A. Luzar and D. Chandler, Nature **379**(6560), 55–57 (1996).
[42] R. Buchner and G. Hefter, Phys. Chem. Chem. Phys. **11**(40), 8984–8999 (2009).
[43] F. Sciortino, A. Geiger, and H. E. Stanley, Nature **354**(6350), 218–221 (1991).
[44] F. S. Csajka and D. Chandler, J. Chem. Phys. **109**(3), 1125–1133 (1998).
[45] A. Luzar, Faraday Discuss. **103**, 29–40 (1996).
[46] D. Laage and J. T. Hynes, Science **311**(5762), 832–835 (2006).
[47] T. C. Berkelbach, H.-S. Lee, and M. E. Tuckerman, Phys. Rev. Lett. **103**(23), 238302 (2009).
[48] M. L. Antipova and V. E. Petrenko, Russ. J. Phys. Chem. A **87**(7), 1170–1174 (2013).
[49] X. Zhang, Q. Zhang, and D.-X. Zhao, Acta Phys.-Chim. Sin. **27**, 2547 (2011).
[50] X.-Z. Li, B. Walker, and A. Michaelides, Proc. Natl. Acad. Sci. U. S. A. **108**(16), 6369–6373 (2011).
[51] J. V. Barth, G. Costantini, and K. Kern, Nature **437**(7059), 671–679 (2005).
[52] A. C. Grimsdale and K. Müllen, Angew. Chem., Int. Ed. **44**(35), 5592–5629 (2005).
[53] A. Krishnamoorthy, M. F. Lin, X. Zhang, C. Weninger, R. Ma, A. Britz, C. S. Tiwary, V. Kochat, A. Apte, J. Yang, S. Park, R. Li, X. Shen, X. Wang, R. Kalia, A. Nakano, F. Shimojo, D. Fritz, U. Bergmann, P. Ajayan, and P. Vashishta, Nano Lett. **19**(8), 4981–4989 (2019).
[54] H. Li, Z. Wang, L. Chen, and X. Huang, Adv. Mater. **21**(45), 4593–4607 (2009).
[55] B. L. Ellis, K. T. Lee, and L. F. Nazar, Chem. Mater. **22**(3), 691–714 (2010).
[56] L. Croguennec and M. R. Palacin, J. Am. Chem. Soc. **137**(9), 3140–3156 (2015).

19 November 2026 22:23:29

© Author(s) 2026

[57]L. Shi and T. Zhao, J. Mater. Chem. A **5**(8), 3735–3758 (2017).
[58]M. C. Payne, M. P. Teter, D. C. Allan, T. A. Arias, and J. D. Joannopoulos, Rev. Mod. Phys. **64**(4), 1045–1097 (1992).
[59]G. Kresse and J. Furthmüller, Phys. Rev. B **54**(16), 11169–11186 (1996).
[60]P. E. Blöchl, Phys. Rev. B **50**(24), 17953–17979 (1994).
[61]P. Hohenberg and W. Kohn, Phys. Rev. **136**(3B), B864–B871 (1964).
[62]W. Kohn and P. Vashishta, *Theory of the Inhomogeneous Electron Gas* (Springer US, 1983), pp. 79–147.
[63]J. Sun, A. Ruzsinszky, and J. P. Perdew, Phys. Rev. Lett. **115**(3), 036402 (2015).
[64]A. Krishnamoorthy, K.-i. Nomura, N. Baradwaj, K. Shimamura, P. Rajak, A. Mishra, S. Fukushima, F. Shimojo, R. Kalia, A. Nakano, and P. Vashishta, Phys. Rev. Lett. **126**(21), 216403 (2021).
[65]R. Ma, N. Baradwaj, K.-i. Nomura, A. Krishnamoorthy, R. K. Kalia, A. Nakano, and P. Vashishta, J. Chem. Phys. **160**(13), 134309 (2024).
[66]D. Semrouni, H.-W. Wang, S. B. Clark, C. I. Pearce, K. Page, G. Schenter, D. J. Wesolowski, A. G. Stack, and A. E. Clark, Phys. Chem. Chem. Phys. **21**(13), 6828–6838 (2019).
[67]P. Vashishta, R. K. Kalia, J. P. Rino, and I. Ebbsjö, Phys. Rev. B **41**(17), 12197–12209 (1990).
[68]G. C. Pimentel and A. L. McClellan, *The Hydrogen Bond* (W.H. Freeman, New York, 1960).
[69]M. Chen, H. Y. Ko, R. C. Remsing, M. F. Calegari Andrade, B. Santra, Z. Sun, A. Selloni, R. Car, M. L. Klein, J. P. Perdew, and X. Wu, Proc. Natl. Acad. Sci. U. S. A. **114**(41), 10846–10851 (2017).
[70]A. Krishnamoorthy, K.-i. Nomura, N. Baradwaj, K. Shimamura, R. Ma, S. Fukushima, F. Shimojo, R. K. Kalia, A. Nakano, and P. Vashishta, J. Phys. Chem. Lett. **13**(30), 7051–7057 (2022).
[71]R. Kumar, J. R. Schmidt, and J. L. Skinner, J. Chem. Phys. **126**(20), 204107 (2007).

19 November 2026 22:23:29

© Author(s) 2026